Science Signaling
AAAS

www.sciencesignaling.org/cgi/content/full/10/501/eaaj1784/DC1

Supplementary Materials for

The matricellular protein TSP1 promotes human and mouse endothelial cell senescence through CD47 and Nox1

Daniel N. Meijles, Sanghamitra Sahoo, Imad Al Ghouleh, Jefferson H. Amaral, Raquel Bienes-Martinez, Heather E. Knupp, Shireen Attaran, John C. Sembrat, Seyed M. Nouraie, Mauricio M. Rojas, Enrico M. Novelli, Mark T. Gladwin, Jeffrey S. Isenberg, Eugenia Cifuentes-Pagano, Patrick J. Pagano*

*Corresponding author. Email: pagano@pitt.edu

Published 17 October 2017, *Sci. Signal.* **10**, eaaj1784 (2017)
DOI: 10.1126/scisignal.aaj1784

This PDF file includes:

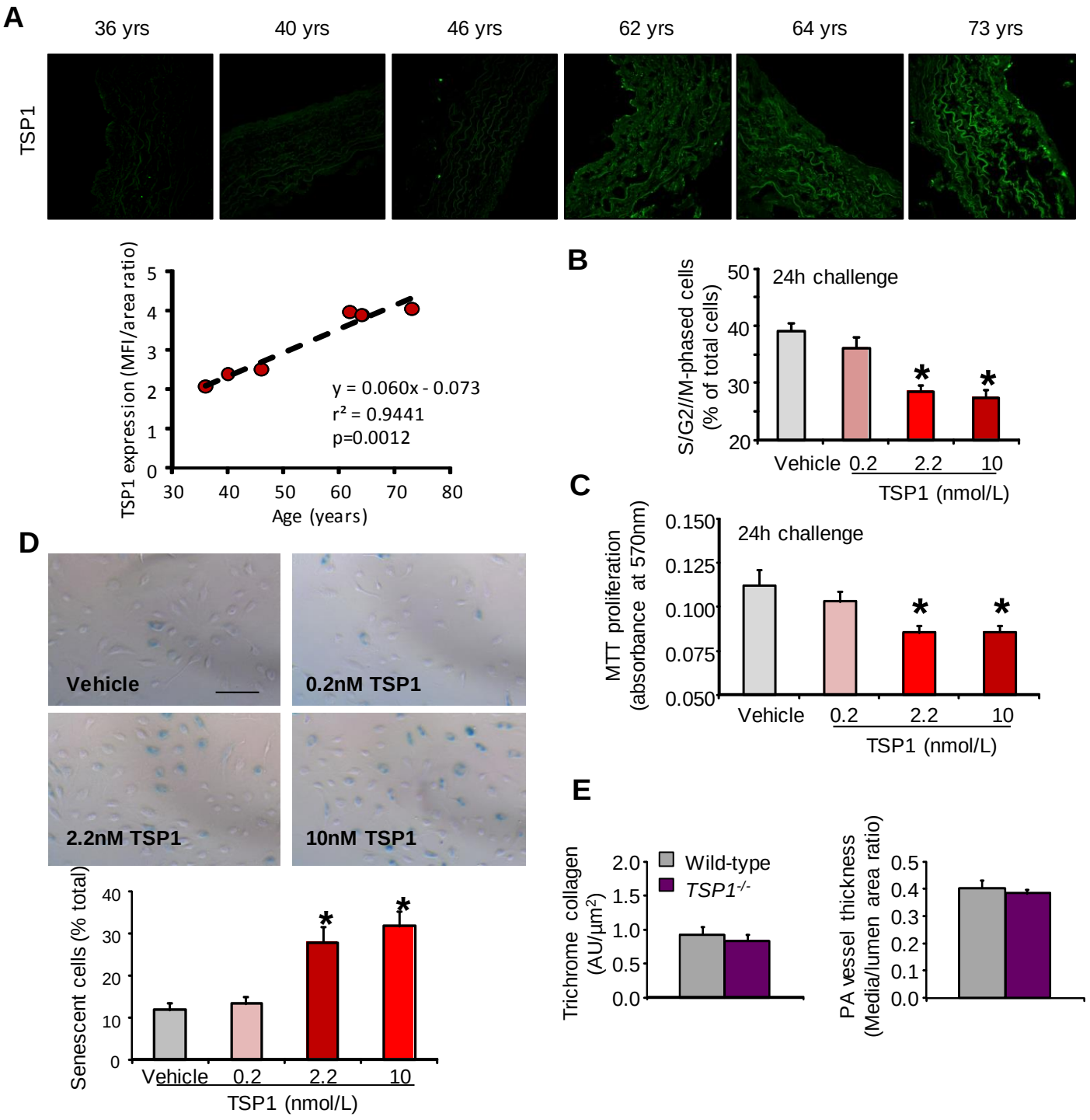

Fig. S1. TSP1 is increased in aging human lung vasculature, and TSP1 exposure reduces endothelial cell proliferation. (**A**) Representative TSP1 abundance in control disease-free human pulmonary artery specimens detected by immunofluorescence (upper panels), measurements of fluorescence intensity (MFI) by ImageJ are plotted as linear regression; equation, r^2 and p values are indicated in the graph *(*lower panel). (**B** and **C**) TSP1 at concentrations of 2.2 and 10 nmol/L inhibit cell cycle progression of HPAECs as characterized by the decreased percent of cells in S/G2/M phases by propidium iodide labeling and FACS (B), and proliferation measured using an ELISA plate-based MTT protocol (C). Data are mean ± SEM (n=4 independent experiments [B] or 3 independent experiments [C]), *p<0.05

compared to vehicle control by one-way ANOVA. (**D**) TSP1 at concentrations of 2.2 and 10 nmol/L promotes HPAEC senescence detected by SA-beta-Gal assay. Bar graph data are mean ± SEM (n=3 independent experiments), *p<0.05 compared to vehicle control by one-way ANOVA. (**E**) *TSP1*$^{-/-}$ mice have similar pulmonary artery vessel collagen (left panel) and thickness (right panel) as wild-type controls at middle age. Data are mean ± SEM (n=3 animals/12 images per group).

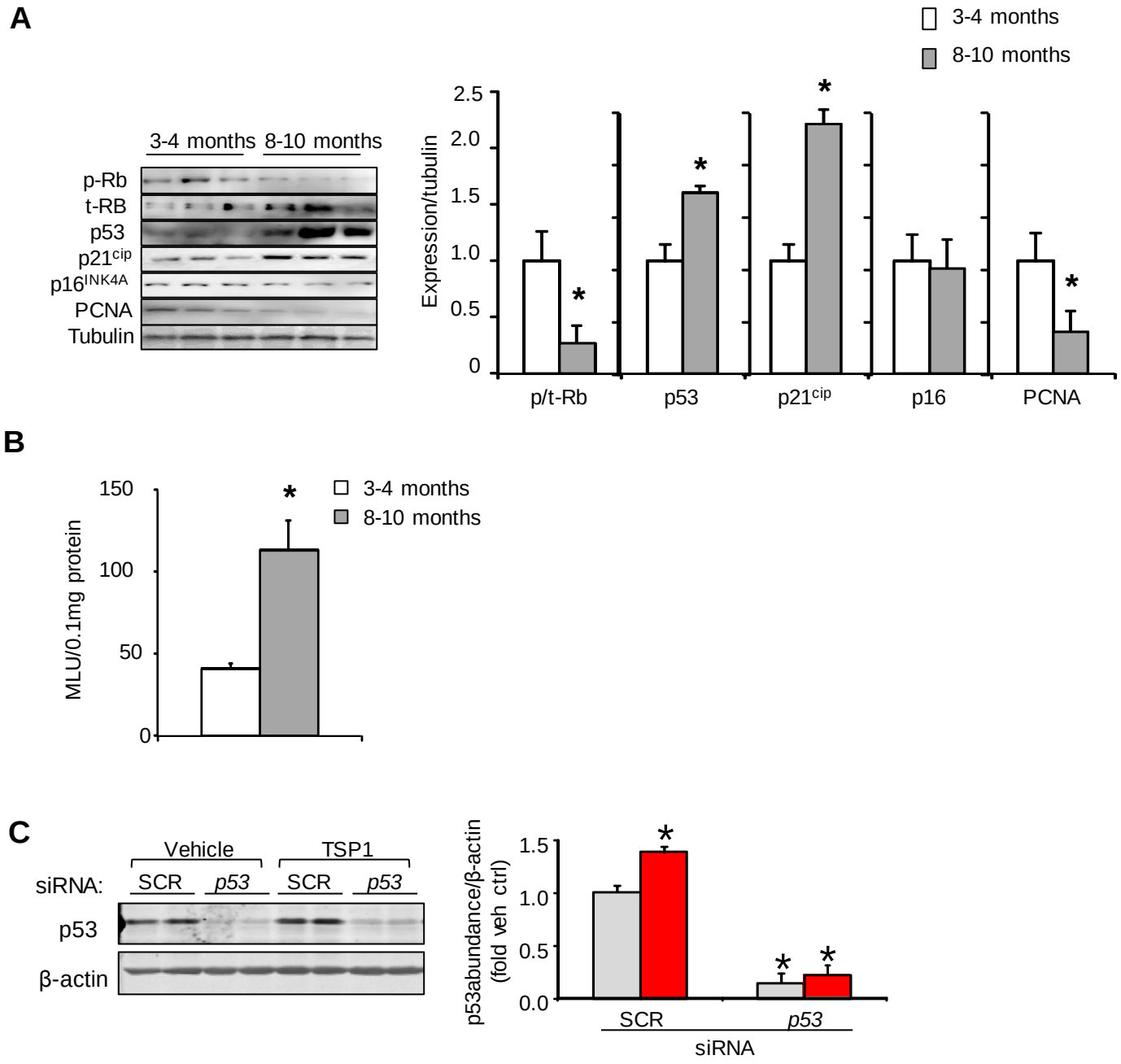

Fig. S2. Age-dependent changes in senescence marker abundance in mice. (**A**) Confirmation that tissue senescence is increased in middle aged mice, consistent with increased p53 and p21^{cip} and decreased Rb phosphorylation and PCNA abundance, with p16INK4A amounts unaffected (Western blot). Graphs are mean ± SEM (n=6 mice per age group), *p<0.05 compared to vehicle control by Students *t*-test for each protein. (**B**) Murine aging increases superoxide production in wild-type animals assayed by lucigenin-enhanced chemiluminescence at middle age. Data are mean ± SEM (n=6 mice per treatment); *p<0.05 compared to vehicle control by Students *t*-test. . (**C**) p53 siRNA knockdown efficiency in HPAEC in the presence of vehicle or TSP1 (2.2 nmol/L; 24h). Left panels: representative Western blots for total-p53 and beta-actin. Right panel:

quantitative analysis of p53 expression; data are mean ± SEM (n=3 independent experiments). *p<0.05 compared to scrambled siRNA (SCR) control by one-way ANOVA.

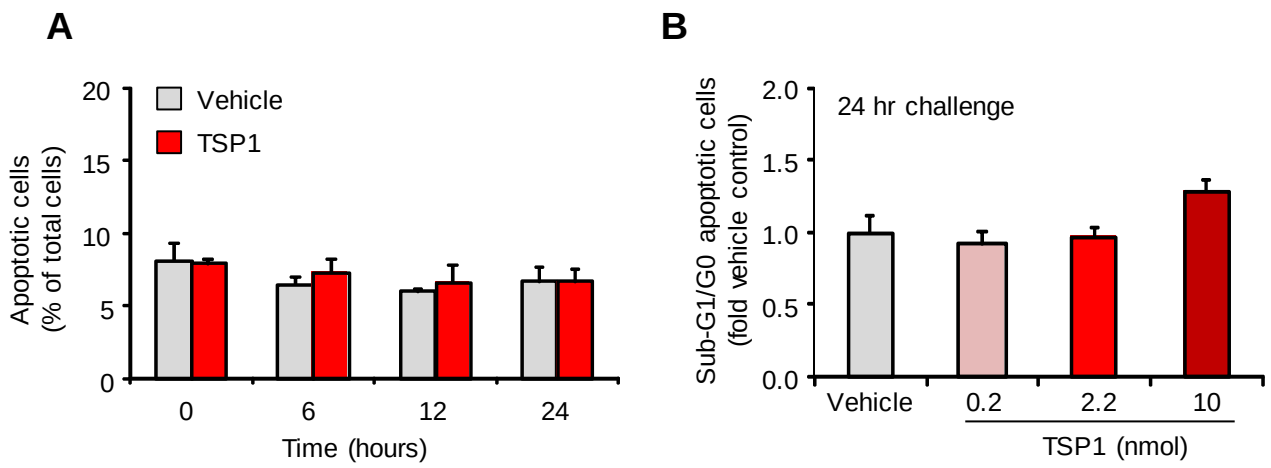

Fig. S3. TSP1 does not induce endothelial cell apoptosis. (**A** and **B**) TSP1 does not induce HPAEC apoptosis at 2.2nmol/L as measured kinetically using trypan-blue inclusion assay (A) or dose-dependently by FACS analysis (B). Data are mean ± SEM (n=3 independent experiments).

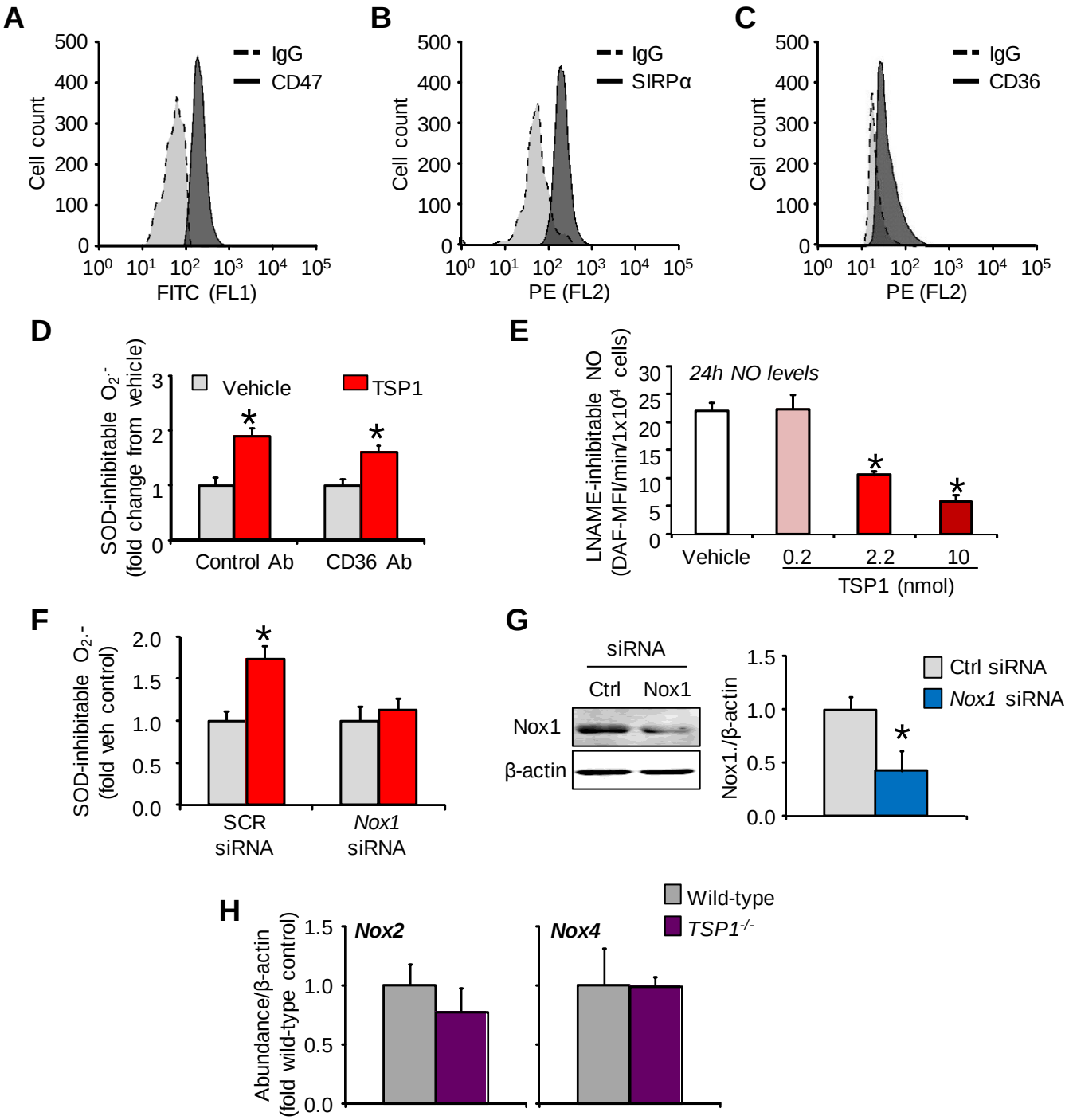

Fig. S4. The TSP1-CD47 axis selectively regulates Nox1. Comparative HPAEC abundance of (**A**) CD47, (**B**) SIRP-α and (**C**) CD36 measured by FACS. Histograms are representative of 3 experiments with 10,000 events recorded per detection. (**D**) CD36 blockade did not inhibit TSP1 induced $O_2^{\cdot-}$ production in HPAECs as measured by cytochrome c reduction. Data are mean ± SEM (n=3 biological replicates per treatment), *p<0.05 compared to vehicle treated controls by one-way ANOVA. (**E**) Effect of TSP1 (24hr) challenge on L-NAME-inhibitable NO production in HPAECs as measured by DAF fluorescence (MFI, mean intensity fluorescence) using a fluorescence plate reader. Data are mean ± SEM (n=3 biological replicates per treatment), *p<0.05 compared to vehicle treated controls by one-way ANOVA. (**F**) *Nox1* gene silencing siRNA inhibits TSP1-induced HPAEC $O_2^{\cdot-}$. Data are mean ± SEM (n=3 biological replicates per treatment), *p<0.05 for TSP1 challenge compared to vehicle control by one-way ANOVA. (**G**) Confirmation of Nox1 knockdown efficiency in HPAECs measured by Western blot. Data are mean ± SEM (n=3 biological replicates per treatment),

*p<0.05 compared to control siRNA by Students *t*-test. (**H**) The abundance of Nox2 and Nox4 in middle-aged wild-type and *TSP1*$^{-/-}$ lungs as measured by Western blot, normalized to β-actin. Data are mean ± SEM (n=6 mice per group).

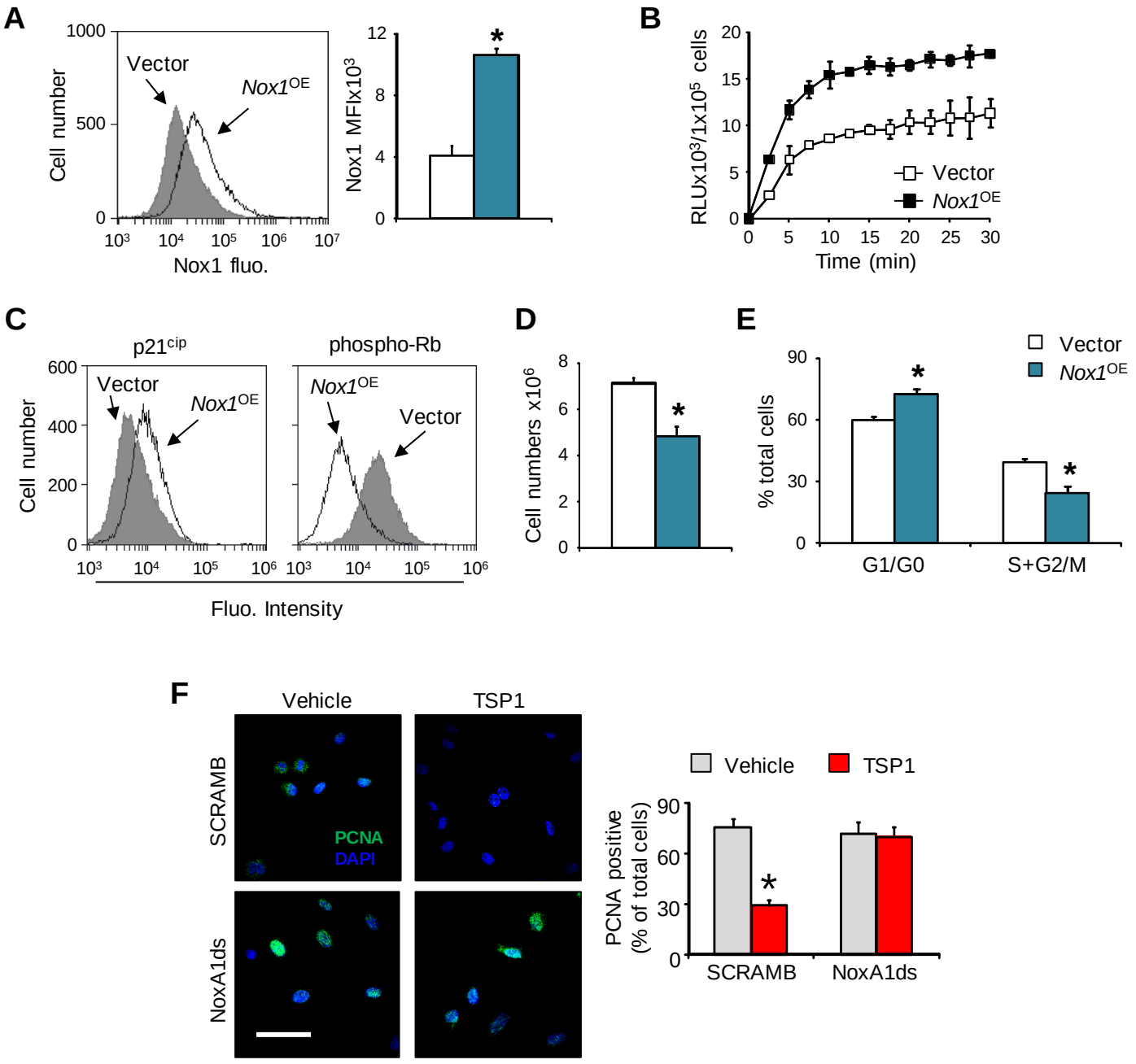

Fig. S5. Nox1 influences cell cycle progression and senescence. Human Nox1 overexpression (Nox1^{OE}) of HPAEC confirmed by FACS detection. Data are mean ± SEM (n=3 independent experiments), *p<0.05 compared to vector controls by Students *t*-test. (**B**) Nox1 overexpression increases $O_2^{\cdot-}$ generation in intact ECs detected by lucigenin-chemiluminescence. Data are mean ± SEM (n=3 independent experiments). (**C**) Nox1 overexpression increases p21^{cip} and decreases Rb phosphorylation detected by FACS labelling. Images are representative of 3 independent experiments. (**D**) Nox1 overexpression decreases EC proliferation assessed by trypan-blue exclusion assay. Data are mean ± SEM (n=3 independent experiments), *p<0.05 compared to vector controls - Students *t*-test. (**E**) Nox1 overexpression decreases cell cycle progression detected by propidium iodide-FACS labelling. Data are mean ± SEM (n=3 independent experiments), *p<0.05 compared to vector controls by Students *t*-test for each phase. (**F**) Treatment of HPAEC with NoxA1ds reverses TSP1-

induced decrease in PCNA expression as assessed by immunofluorescence (PCNA, green; DAPI, blue). Data are mean ± SEM (n=3; 12-20 images per group; scale bar: 10μm); *p<0.05 for TSP1 challenge compared to SCRAMB vehicle control by one-way ANOVA.

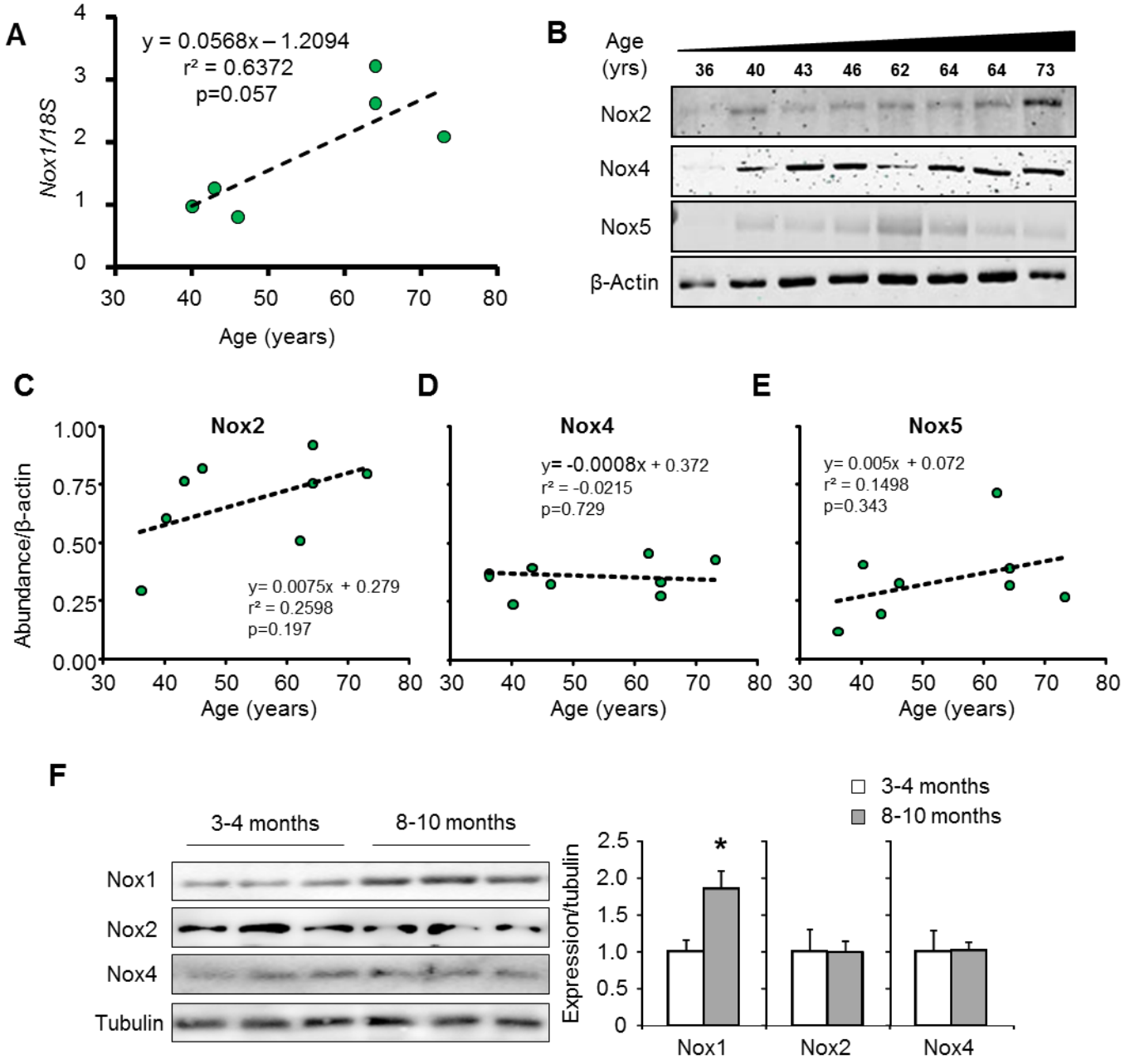

Fig. S6. Age-dependent changes in Nox isoform abundance in human and mice lung samples. (**A**) Expression of *Nox1* mRNA significantly correlated with age in human lung homogenates as quantified by qRT-PCR. (**B** to **E**) Nox2, Nox4 and Nox5 protein abundance in the lungs of humans of various ages (B) normalized to beta-actin (C-E) as assessed by Western blot. Data are plotted as linear regression and equation,

r^2 and p values are indicated in the corresponding graphs. (**F**) Expression of Nox1, Nox2 and Nox4 protein in aging murine lungs assessed by Western blot (left panels) normalized to alpha-tubulin (right panels). Data are mean ± SEM (n=6 mice per age group); *p<0.05 compared to vector controls by Students *t*-test for each protein.

Table 1. Characteristics of pulmonary disease–free human samples.

Parameter	<50 yrs (n=4)	>50 yrs (n=4)
Mean age (SEM)	41.25 ± 2.13	65.75 ± 2.46
Range (years)	36 - 46 (10)	62 - 73 (11)
Male gender (%)	100	50
Smoking history	1/4	0/4
Av BMI (kg/m^2)	31.0 ± 1.6	32.3 ± 3.3

Supplementary Table 2: Cause of death and existence of nonpulmonary diseases of the human samples.

Cause of Death	Number (>50 yrs)
Stroke	4/8 (3/4)
Blunt trauma	4/8 (1/4)
Associated Systemic Diseases	Number (>50 yrs)
Systemic hypertension*	4/8 (3/4)
Diabetes*	2/8 (1/4)

*denotes evidence of treated systemic disease and not cause of death.
( ) denote ratios in subjects greater than 50 years of age.